Advanced Composite Materials

ISSN: 0924-3046 (Print) 1568-5519 (Online) Journal homepage: http://www.tandfonline.com/loi/tacm20

Damage characterization and numerical modeling of titanium matrix composites subjected to low-velocity impact for landing gear application

Tomohiro Yokozeki, Naoki Kotsuka, Keisuke Yoshida, Kouta Fujiwara & Toyohiro Sato

To cite this article: Tomohiro Yokozeki, Naoki Kotsuka, Keisuke Yoshida, Kouta Fujiwara & Toyohiro Sato (2015) Damage characterization and numerical modeling of titanium matrix composites subjected to low-velocity impact for landing gear application, Advanced Composite Materials, 24:4, 343-358, DOI: 10.1080/09243046.2014.912412

To link to this article: http://dx.doi.org/10.1080/09243046.2014.912412

Published online: 24 Apr 2014.

Advanced Composite Materials, 2015
Vol. 24, No. 4, 343–358, http://dx.doi.org/10.1080/09243046.2014.912412

Damage characterization and numerical modeling of titanium matrix composites subjected to low-velocity impact for landing gear application

Tomohiro Yokozeki[a]*, Naoki Kotsuka[a], Keisuke Yoshida[a], Kouta Fujiwara[b] and Toyohiro Sato[b]

[a]*Department of Aeronautics and Astronautics, The University of Tokyo, Tokyo, Japan;* [b]*Research Department, Sumitomo Precision Products Co., Ltd, Hyogo, Japan*

(*Received 20 January 2014; accepted 3 April 2014*)

Titanium matrix composites (TMCs) is considered as a candidate material for landing gear structures of the aircraft, which requires the damage tolerant consideration. In order to investigate the damage behavior of SiC-fiber/titanium matrix composites subjected to foreign object impact, low-velocity impact experiments are conducted. Finite element modeling to simulate the damage behavior of TMCs is developed considering the plastic deformation and the damages. Numerical results of mechanical response and damage behavior are compared with experimental results. It is shown that the developed modeling can capture the impact damage of TMCs. In the last part of the present study, a prototype of TMC landing gear structure is fabricated. Impact damage behavior and residual compressive strength are evaluated, and the results are compared with numerical simulation.

Keywords: metal matrix composites (MMCs); damage tolerance; impact behavior; finite element analysis (FEA)

1. Introduction

Aircraft landing gear components generally occupy about 4% of the entire weight of aircraft, although they are not used during the flight. Current landing gear structures are mainly made of high strength steel (e.g. 300 M [1]). Corrosion and fatigue problems of such materials may occur in service, which result in increase in cost and labor to control the manufacturing quality and maintenance program. Therefore, new types of landing gear structures are demanded to avoid the above-mentioned problems. High strength titanium alloy has been used to reduce both the cost of maintenance and cost of ownership by increased corrosion resistance and reduced structural weight. Another feasible candidate to replace high strength steel is carbon fiber-reinforced plastic (CFRP) composite with high specific stiffness and strength, as seen in the side braces of main landing gear of Boeing 787-8 aircraft. Our preliminary study [2] indicates that application of CFRP to landing gear results in increase of the volume of landing gear components, which may possibly induce the weight of the total aircraft. In addition, very thick CFRPs are required for landing gear components, and low bearing strength and inspection problem are to be solved for the real application.

*Corresponding author. Email: yokozeki@aastr.t.u-tokyo.ac.jp

In this paper, application of titanium matrix composites (TMC), especially continuous SiC-fiber/Titanium matrix (SiC/Ti) composites, is considered as an alternative candidate material for landing gear structures. SiC/Ti composites have capability of reducing structural weight owing to high-specific stiffness and strength. In addition, use of TMC is expected to mitigate the risk of corrosion compared to high strength steel and the lightning strike damage compared to CFRPs. As it has been expected that SiC/Ti composites are useful for gas turbine engine components,[3,4] numerous studies have been performed focusing on static tensile properties,[5,6] fiber/matrix interface properties,[7–10] fatigue life, damage mechanism,[11–14] thermal fatigue,[15] creep, [16,17] etc. However, in order to apply TMCs to the landing gear components, consideration of foreign object damages (FOD, e.g. stones on the ground, falling tools and bolts, tire debris, etc.) is required [18] in a similar manner of CFRPs.[19,20] Virtual testing technology for the assessment of damage and strength of SiC/Ti composites is also necessary to avoid the cost/labor increase in the development and certification procedures.

This paper focuses on the experimental characterization of low-velocity impact damage in SiC/Ti composites, and the development of simplified numerical simulation method which is applicable to SiC/Ti structures. Damage behavior of SiC/Ti composites owing to low-velocity transverse impact are identified, and then, damage and plasticity models accounting for the observed damage mechanism of SiC/Ti composites are incorporated in the commercial finite element code. The simulated damage behavior is compared with the experimental observation to validate the present numerical model. Finally, a prototype of side brace structure is fabricated. Impact damage behavior and residual compressive strength are characterized, and compared with numerical simulation.

2. Experimental

In the present study, SiC/Ti unidirectional composites are of interest for landing gear application. This is because landing gear structures (e.g. side braces) are mainly subject to uniaxial compression and tension, and titanium matrix is considered to be stiff enough to maintain the stability against the compressive loading. As the titanium alloy layer is expected to mitigate the damage of brittle composites,[21] two kinds of SiC/Ti plates (with and without titanium clad layers) are prepared to investigate the damage behavior under transverse impact loads. The followings sections describe the material used, mechanical tests for basic mechanical properties, and low-velocity impact tests of TMC composites.

2.1. Material

This study utilized unidirectional TMC composites consisting SiC fibers and titanium (Ti-3Al-2.5V) matrix fabricated by Hot Isostatic Pressing (HIP) process. The fiber diameter was about 100 μm, and the fiber volume fraction of SiC/Ti was about 33%. In order to improve the damage resistance property, SiC/Ti composites covered by titanium (Ti-6Al-4V) clad layers were also fabricated. The resultant thickness of TMC plates was about 3 mm for SiC/Ti without clad layer, and about 3.8 mm for SiC/Ti with clad layers (i.e. SiC/Ti with 3.0 mm thickness and two clad layers with 0.4 mm thickness). A cross-sectional image of the prepared SiC/Ti plate with clad layers is shown in Figure 1.

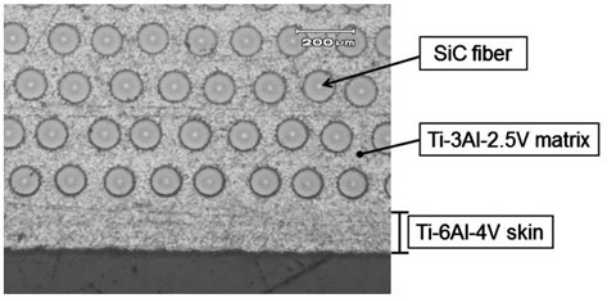

Figure 1. Cross-sectional view of SiC/Ti with clad layer.

Table 1. Mechanical properties of SiC/Ti.

Density	4090 kg/m^3
Stiffness (0°) E_x	185 GPa
Stiffness (90°) E_y	119 GPa
Shear stiffness (in-plane) G_{xy}	46.4 GPa
Shear stiffness G_{yz}	45.9 GPa*
Poisson's ratio v_{xy}	0.32
Poisson's ratio v_{yz}	0.30*
Yield stress (0°)	510 MPa
Strength (0°) X_t	1481 MPa
Yield stress (90°)	202 MPa
Strength (90°) Y_t	414 MPa
Yield shear stress (in-plane)	115 MPa
Shear Strength (in-plane)	220 MPa

*Estimated value.

Table 2. Mechanical properties of Ti-6Al-4V.

Density	4430 kg/m^3
Stiffness E	126 GPa
Poisson's ratio v	0.35
Yield stress	700 MPa
Strength	940 MPa

The authors evaluated the basic mechanical properties of SiC/Ti composites and clad layers based on tensile tests.[22,23] The elastic moduli and strength properties of SiC/Ti and Ti-6Al-4V are summarized in Tables 1 and 2, respectively. It should be noted that SiC/Ti composites exhibit plastic deformation (even in 0° direction), and nonlinear stress–strain relations were obtained. Elastic moduli were evaluated in the linear region of stress–strain curves. This study defined the yield stress as the stress when the nonlinear deformation exhibits. Nonlinear region of the curve was utilized for plastic modeling.

2.2. *Low-velocity impact test*

The drop-weight low-velocity impact tests were conducted to TMC specimens with 100 mm length and 75 mm width using Instron Dynatup 9250HV. Experimental setup is shown in Figure 2. A specimen was sandwiched by the fixture with 80 mm × 60 mm

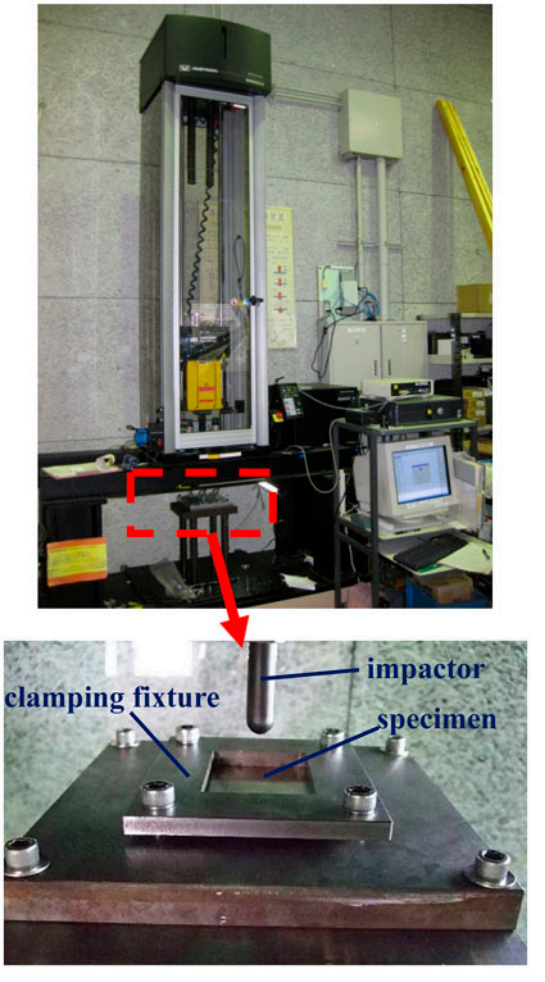

Figure 2. Drop-weight impact test apparatus of TMC specimens.

rectangular hole, and was clamped by lightly tightening the bolts on the four corners of the fixture (Figure 2). Impact load was applied to the specimens by the fall of the impactor with hemispherical steel tip, whose diameter was 15.9 mm, at the center of the specimens. The total mass of the impactor was 15.56 kg. Sic fiber direction coincided with the longitudinal direction. Three levels of impact loading (impact energy of 20, 45, and 70 J) were applied to the TMC specimens.

After the impact events, ultrasonic inspection was performed to investigate the inner damage behavior of TMC composites. Nonlinear resonant ultrasonic method [24] was applied in this study. Some specimens were also cut to observe the damages by the optical microscope.

2.3. *Impact damage characterization*

The reaction forces of the impactor were recorded during the impact test. The corresponding accelerations and displacements of the impactor were also calculated in the

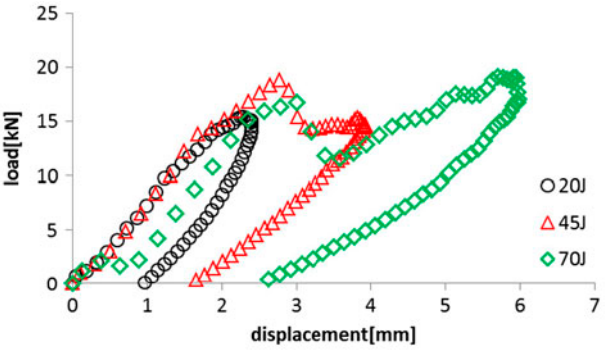

Figure 3. Impact force–displacement curve of SiC/Ti composites with clad layers.

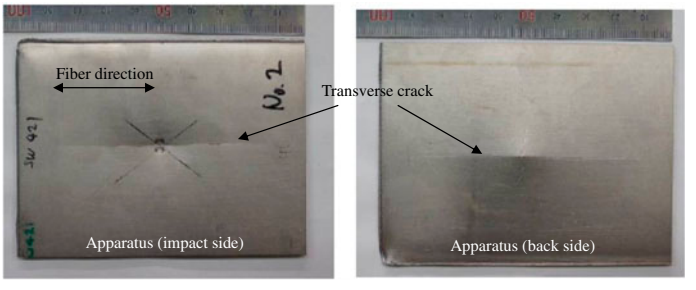

Figure 4. Impact damage of SiC/Ti without clad layer subjected to 45 J impact.

data acquisition system. Figure 3 shows the measured impact force–displacement curves corresponding to 20, 45, and 70 J impacts to TMC composites with clad layers. The apparatus of impacted specimens is shown in Figure 4 for TMC composites without clad layer subjected to 45 J impact, and in Figure 5 for TMC composites with clad layers subjected to 45 J impact. Transverse crack along fiber direction and visible residual deformation near the impact point can be recognized. Apparently, clad layers act as a role to mitigate the impact damages.

Impact-induced inner damages were also observed by the ultrasonic inspection and the optical microscope. Figure 6 shows a cross-sectional view of the TMC specimen without clad layer (subject to 20 J impact) near the impact point, in which SiC fibers

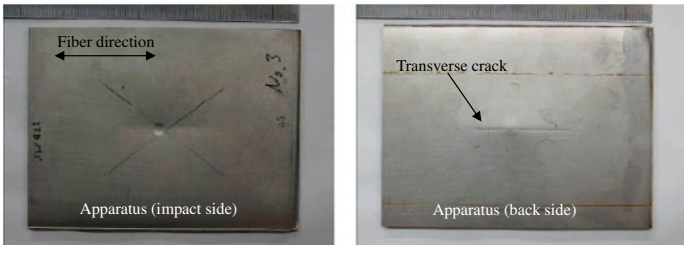

Figure 5. Impact damage of SiC/Ti with clad layers subjected to 45 J impact.

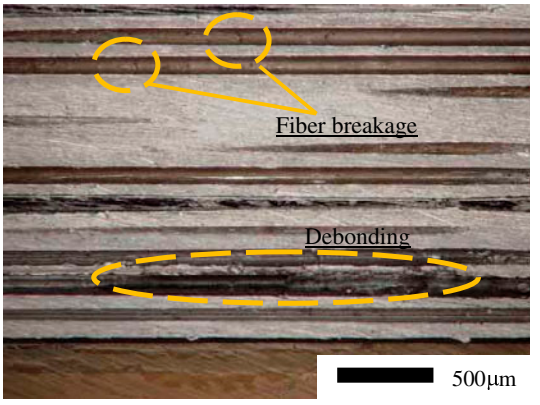

Figure 6. Cross-sectional view of the impacted SiC/Ti.

align to the horizontal direction. Fiber breakages and fiber/matrix debondings are identified. Ultrasonic inspection results (projected images) for TMCs without clad layer are summarized in Figure 7(a), which indicates a major transverse crack along the fiber direction, as well as elliptical damages near the impact point. Impact damages of TMCs with clad layers are also shown in Figure 7(b). It is indicated that damage trends are similar, but impact-induced damages are significantly mitigated owing to clad layers.

Combination of specimen apparatus, optical cross-sectional observation, and ultrasonic inspection results of impacted specimens suggests that impact damage mechanisms of TMC plates are classified as summarized below.

- A major transverse crack along SiC fiber direction.
- Fiber breakages and fiber/matrix debondings in the elliptic zone near the impact point.

Plastic deformation in TMCs and clad layers was also recognized. The following section describes numerical model to simulate the impact damages of TMCs, taking these damage mechanisms into account.

3. Damage simulation

3.1. Material modeling

When TMCs specimens are subjected to impact loadings, TMCs exhibit complex damage accumulation consisting of yieldings, fiber/matrix debondings, fiber fractures, and major transverse crackings. To simplify such complex interaction between damage and plasticity in SiC/Ti, the present analysis incorporates the following modelings: (i) the plastic modeling taking yielding and fiber/matrix debonding into account and (ii) the strength-based damage onset and resulting stiffness degradation to express fiber fractures and major transverse cracks. The analysis also includes plastic deformation of titanium clad layers. The above-mentioned plastic and damage models are incorporated in the commercial finite element code (MSC Marc). SiC/Ti and clad layers are treated as homogeneous anisotropic (but transversely isotropic) materials and isotropic materials, respectively, and the representative properties are shown in Tables 1 and 2.

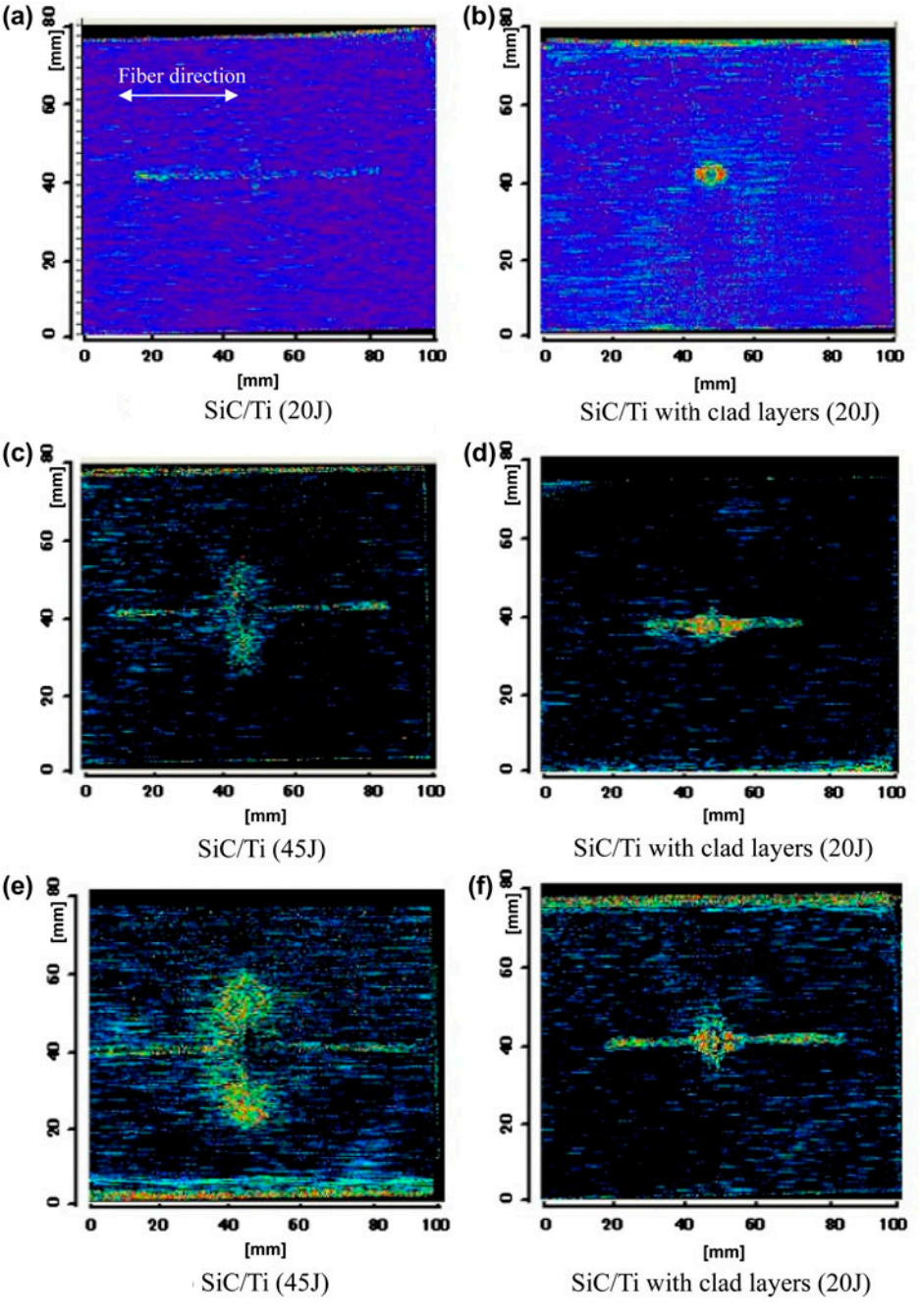

Figure 7. Ultrasonic inspection results (projected images) of impacted specimens.

Hill and Mises yield functions are used for SiC/Ti and clad layers, respectively. Yield stresses and plastic hardening curves were determined based on the tensile test results as described in Section 2.1 and Ref. [23]. The used plastic parameters and hardening curves are summarized in Appendix 1. In order to incorporate the possible fiber

failure and major transverse cracking of SiC/Ti into the models, the following simple failure criterion is selected as,

$$\sigma_x = X_t, \quad \sigma_y = Y_t \tag{1}$$

where X_t is tensile strength in 0° direction of SiC/Ti, Y_t is tensile strength in 90° direction of SiC/Ti, σ_x and σ_y are stress component of the elements in the fiber direction and transverse direction, respectively. Once the element failure is judged, all stiffness constants reduce to 1% of their original values to express the catastrophic failure of fiber breakage and major transverse cracking in SiC/Ti. It is assumed that SiC/Ti shows no stiffness degradation except for these catastrophic failure modes, and material nonlinearity of SiC/Ti and clad layers is caused only by plasticity. The transverse crack in clad layers is also incorporated by elimination of node constraints when the stress component reaches the strength value of titanium (Ti-6Al-4V), which is similar to Equation (1).

3.2. *Low-velocity impact damage simulation*

Numerical damage simulation on the drop-weight impact tests of TMC specimens is conducted herein. Considering calculation cost required, the finite element models had a reduced 1/4 part of the experiments for specimens. Out-of-plane displacements of nodes which contact the clamping fixtures were fixed to zero. The impactor was modeled as stiff elements which have same mass, stiffness, and tip shape as the experiment. An example of the finite element model is shown in Figure 8. As the authors expect to use the same model for dynamic high-speed impact simulation in the future study, dynamic simulation was performed for the present low-velocity impact using the single-step Houbolt implicit method. The time steps were properly shortened at the increments when the convergence was difficult.

3.3. *Simulation results*

Simulated impact force history of TMCs subjected to 45 J impact is presented in Figure 9 in comparison with experimental time history. The figure suggests good agreement between the simulated results and the experimental data. The experimental and numerical results are, however, somewhat different during unloading process. This discrepancy comes from the material model adopted in this study. The present analysis

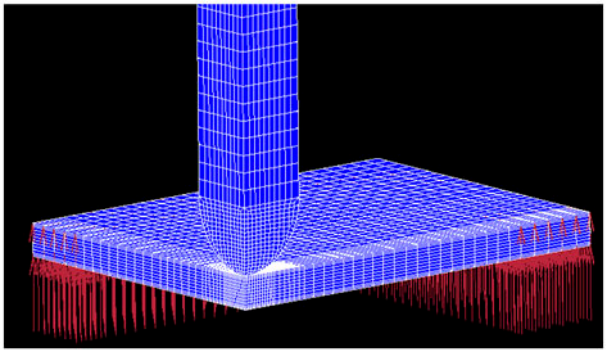

Figure 8. Finite element model for low-velocity impact simulation (1/4 model for SiC/Ti).

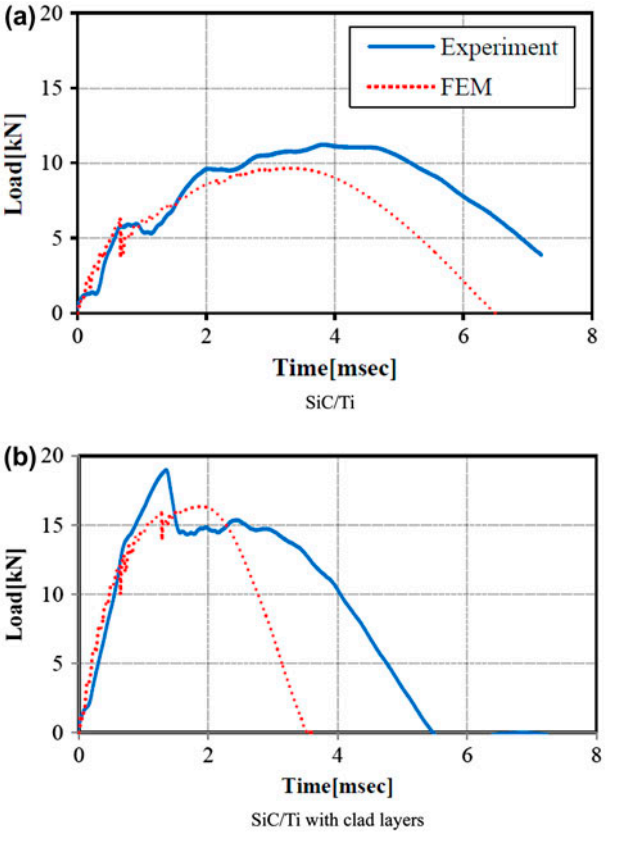

Figure 9. Impact force history of TMCs subjected to 45 J impact.

does not consider stiffness degradation due to minute damages before catastrophic failure, resulting in overestimate of the residual stiffness during unloading process. Figure 9 indicates that the present simplified model can estimate the mechanical behavior during loading process even though the unloading behavior is somewhat inaccurate. Therefore, the authors consider that the present simplified model is useful to predict the damage accumulation of TMCs.

The simulated damage area after the impact corresponding to Figure 9 is shown in Figure 10. In this figure, colored elements indicate the plastically deformed elements in SiC/Ti with equivalent plastic strains over 0.26% (catastrophically damaged elements are included). Because of the simplified method with respect to material modeling, minute damages like fiber/matrix debonding are not able to appear as damaged elements in the calculated results. On the other hand, such minute damages have a close relation to equivalent plastic strain in this model. Comparison with experimental damage behavior determined the threshold of equivalent plastic strain as mentioned above. The numerical simulation agrees well with the experimental damage trend. The numerical model can capture the damage modes including major transverse crack along fiber direction and elliptic damages near the impact point. In addition, the analysis shows the mitigation of impact damage owing to clad layers clearly.

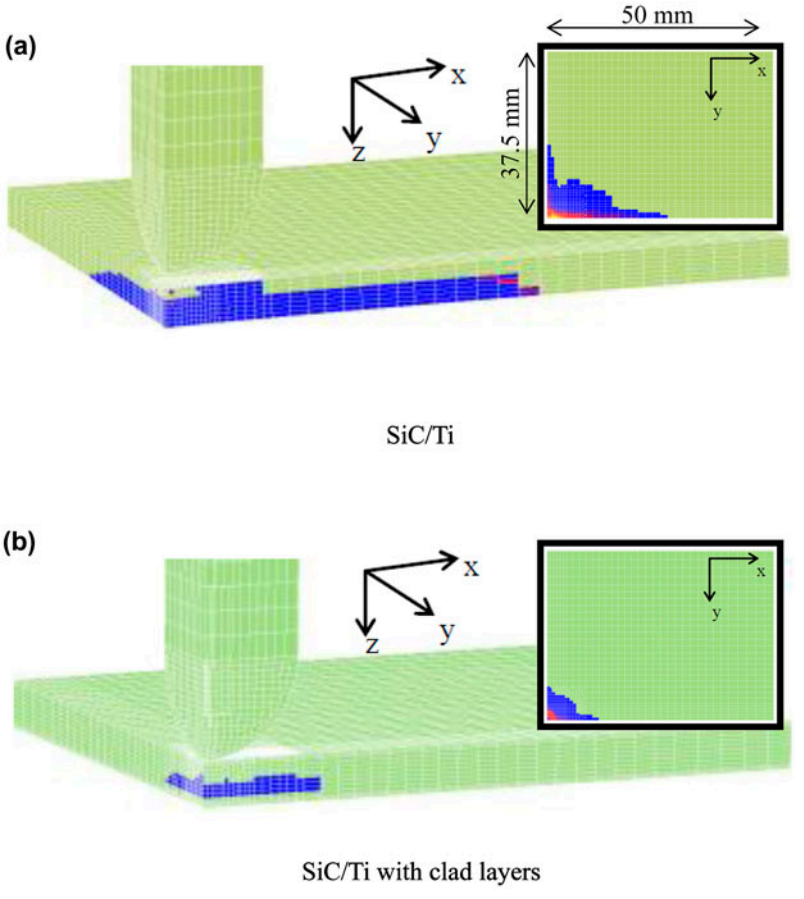

Figure 10. Simulated damage elements by 45 J impact (magnified images surrounded by solid lines indicate projected damage areas).

The projected damage areas predicted by the simulation are summarized in comparison with the experimental ultrasonic results in Table 3. The predicted damage areas show relatively good agreement with the experimental results, especially for SiC/Ti without clad layers. Although the accuracy of the numerical simulation for SiC/Ti with clad layers is to be improved, the simplified numerical model predicts the damage

Table 3. Comparison of projected damage area.

Specimen	Impact energy (J)	Damage area (mm^2) (simulation)	Damage area (mm^2) (experiment)
SiC/Ti	20	196	192
	45	548	548
	70	1140	997
SiC/Ti with clad layers	20	51	52
	45	132	187
	70	207	279

modes of SiC/Ti composites, damage mitigation by clad layers, and the damage area by impact loading with intermediate accuracy. The present numerical model can be directly applied to high-velocity impact, and application of the model to high-velocity impact simulation and structural design of landing gear structures is ongoing.

4. Application to the prototype of side brace structure

Prototype of landing gear structure using TMC has been fabricated as shown in Figure 11. This is assumed as a side brace member in the landing gear structures. It should be noted that structural weight could be reduced by about 30% using TMCs compared to the conventional high-strength steel structure. The cylindrical section had the external diameter of 60 mm, and consisted of SiC/Ti (2 mm thickness) covered by inner and outer clad layers (0.5 mm thickness for each layer). The total length was 800 mm, and the rest of the part was made of titanium (Ti-3Al-2.5V). This prototype was integrally fabricated by HIP process, and the precise machining was applied to the product.

Low-velocity impact was applied to the central section of the prototype as shown in Figure 12. The impactor has cylindrical tip with a diameter of 15.9 mm and with a length of 60 mm. Impact energy level was set as 40 J. The supporting condition of the prototype was almost simply supported using the bearing joints.

The apparatus of impact damage is shown in Figure 13(a), while the simulated damage (plastic strain plot) calculated by the present FEM analysis is indicated in

Figure 11. Prototype of TMC side brace structure.

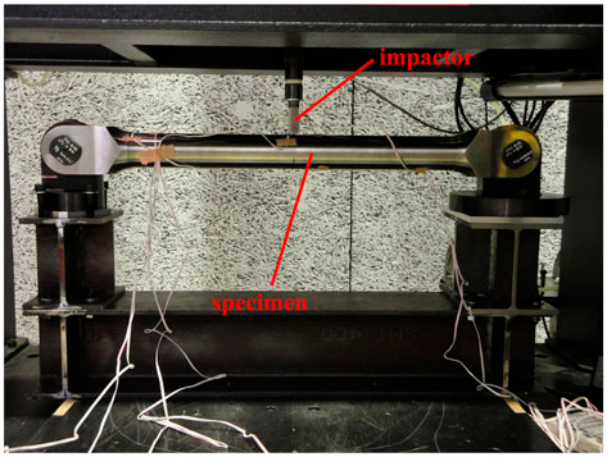

Figure 12. Impact test setup of TMC side brace structure.

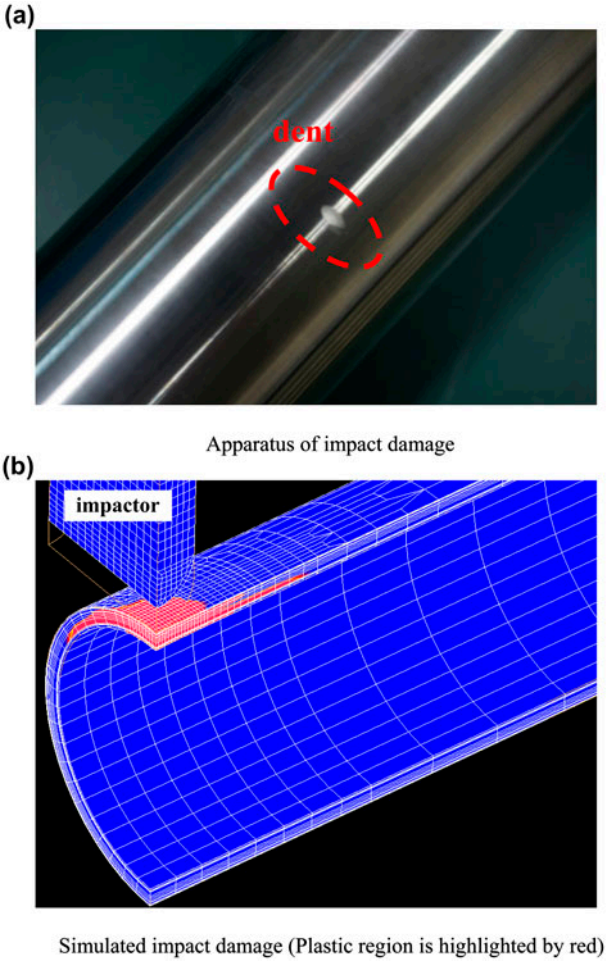

Figure 13. Experimental and simulated impact damage of side brace structure subjected to 40 J impact.

Figure 13(b). Small size residual deformation at the impact point was identified in the experiment. The visible dent takes the form of ellipse with about 7 mm major axis (hoop direction) and 3 mm minor axis (axial direction). Numerical simulation also predicted the small size plastic deformation (about 22 mm in hoop direction and 18 mm in axial direction). Figure 13(a) shows the visible dent, and plastic deformation region is considered to be several times larger than the visible dent size. It can be concluded that numerical plastic strain plot agrees well with the experimental observation.

Finally, axial compressive test was performed using the impacted side brace structure. Bearing joints were also utilized in the compressive test. In the experiment, the buckling load of impacted structure was 734 kN, while intact structure had the buckling load of 785 kN. No major structural degradation (only about 6% reduction of buckling load) owing to 40 J impact was observed compared to intact structure.[2] To simulate this phenomenon, nonlinear analysis of the side brace structure with simulated impact damages (corresponding to Figure 13(b)) under compressive loading was conducted.

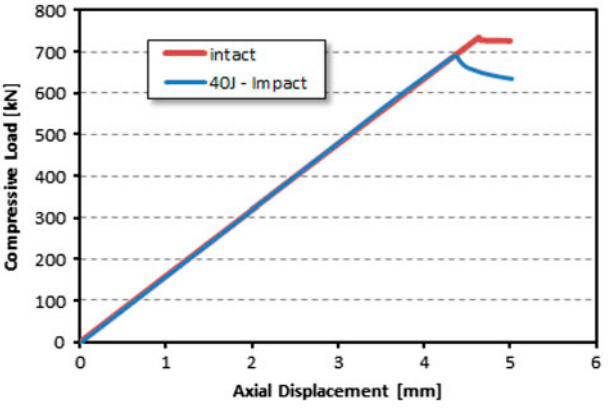

Figure 14. Comparison of numerical load-displacement (axial displacement) curves between impact-damaged and intact structures.

The numerical load-displacement (axial displacement) curves are compared between impact-damaged and intact structures in Figure 14. Only 5% reduction of maximum compressive load was simulated in comparison to the intact side brace structure. This result indicates the validity of the numerical model. It was demonstrated that the numerical model can simulate the impact damage behavior of TMC landing gear structure, and is useful for damage tolerant design of TMC structures.

5. Conclusions

The present paper described the experimental characterization of low-velocity impact damage in SiC/Ti composites and the numerical model to predict the damage evolution in SiC/Ti composites. Low-velocity impact damages consisted of yielding, fiber-matrix debonding, fiber breakage, and major transverse cracking. Clad titanium layers played an important role to reduce the impact damage accumulation in SiC/Ti composites.

To simulate the impact damage behavior, numerical simplified damage model was developed. Plasticity model accounted for minute damages including material yielding and fiber-matrix debondings, and stiffness reduction was taken into account for tensile fiber breakage and major transverse cracking. The simulated results of impact response during loading and damaged area agreed well with the experimental results. The numerical results also showed damage modes and the effect of clad layers that are similar to the experimental observation.

Finally, a prototype of landing gear structure was fabricated and subjected to impact and compressive tests. Numerical simulation could predict the small size plastic deformation of TMC structure in the case of 40 J impact, which agreed well with the experimental observation. It was demonstrated that the numerical model can simulate the impact damage behavior of TMC landing gear structure, and is useful for damage tolerant design of TMC structures. It is expected that the observed findings of damages in TMCs and the developed simple numerical model are helpful for the future development of TMC landing gear structures.

Acknowledgement

The authors would like to thank Dr E. Hara in Japanese Aerospace Exploration Agency for the support of the present experimental study.

References

[1] SAE AMS6257D. Steel bars, forgings, and tubing 1.6Si-0.82Cr-1.8Ni-0.40Mo-0.08 V(0.40-0.44C) consumable electrode vacuum remelted normalized and tempered. Warrendale: SAE International; 2007.
[2] Takahashi N, Sato T, Nakatsuka S, Fujiwara K, Yoshida K, Yokozeki T. Titanium metal matrix composite development for commercial aircraft landing gear structure. In: Proceedings of 28th International Congress on the Aeronautical Sciences, CD-ROM; Brisbane; 2012.
[3] Lindroos VK, Talvitie MJ. Recent advances in metal matrix composites. J. Mater. Process. Technol. 1995;53:273–284.
[4] Leyens C, Hausmann J, Kumpfert J. Continuous fiber reinforced titanium matrix composites: Fabrication, properties and applications. Adv. Eng. Mater. 2003;5:399–410.
[5] Jeng SM, Yang JM, Yang CJ. Fracture mechanisms of fiber-reinforced titanium alloy matrix composites part II: Tensile behavior. Mat. Sci. Eng. 1991;A138:169–180.
[6] Gundel DB, Wawner FE. Experimental and theoretical assessment of the longitudinal tensile strength of unidirectional SiC-fiber/Titanium-matrix composites. Compos. Sci. Technol. 1997;57:471–481.
[7] Yang CJ, Jeng SM, Yang JM. Interfacial properties measurement for SiC fiber-reinforced titanium alloy composites. Scr. Metall. Mater. 1990;24:469–474.
[8] Yang JM, Jeng SM, Yang CJ. Fracture mechanisms of fiber-reinforced titanium alloy matrix composites part I: Interfacial behavior. Mat. Sci. Eng. 1991;A138:155–167.
[9] Matikas TE. High temperature fiber fragmentation characteristics of SiC single-fiber composite with titanium matrices. Adv. Compos. Mater. 2008;17:75–87.
[10] Mortensen A, Llorca J. Metal matrix composites. Annu. Rev. Mater. Res. 2010;40:243–270.
[11] Talreja R. A conceptual framework for interpretation of MMC fatigue. Mat. Sci. Eng. 1995; A200:21–28.
[12] Jeng SM, Alassoeur P, Yang JM. Fracture mechanisms of fiber-reinforced titanium alloy matrix composites part IV: Low cycle fatigue. Mat. Sci. Eng. 1991;A148:67–77.
[13] Gabb TP, Gayda J, Mackey RA. Isothermal and nonisothermal fatigue behavior of a metal matrix composite. J. Compos. Mater. 1990;24:667–686.
[14] Nicholas T. An approach to fatigue life modeling in titanium-matrix composites. Mat. Sci. Eng. 1995;A200:29–37.
[15] Park YH, Marcus HL. Influence of interface degradation and environment on the thermal and fracture fatigue properties of titanium-matrix/continuous SiC-fiber composites. In: Hack JE, Amateau MF, editors. Mechanical behavior of metal-matrix composites. New York: Metallurgical Society of AIME; 1983. p. 65–75.
[16] Jeng SM, Yang JM. Creep behavior and damage mechanisms of SiC-fiber-reinforced titanium matrix composite. Mat. Sci. Eng. 1993;A171:65–75.
[17] Weber CH, Du ZZ, Zok FW. High temperature deformation and fracture of a fiber reinforced titanium matrix composite. Acta Mater. 1996;44:683–695.
[18] SAE AIR5552. Development and qualification of composite landing gear. Warrendale: SAE International; 2010.
[19] Ogasawara T, Sugimoto S, Kato H, Ishikawa T. Fatigue behavior and lifetime distribution of impact-damage carbon fiber/toughened epoxy composites under compressive loading. Adv. Compos. Mater. 2013;22:65–78.
[20] Ogi K, Kim J-W, Ono K, Uda N. Impact damage and residual tensile strength of a CF-SMC composite. Adv. Compos. Mater. 2013;22:29–47.
[21] Ogasawara T, Arai N, Fukumoto R, Ogawa T, Yokozeki T, Yoshimura A. Titanium alloy foil-inserted carbon fiber/epoxy composites for cryogenic propellant tank application. Adv. Compos. Mater. 2014;23:129–149.
[22] Yoshida K, Yokozeki T, Fujiwara K, Sato T. Numerical evaluation of foreign object damage in SiC fiber/titanium composite. In: Proceedings of 12th Japan International SAMPE Symposium, CD-ROM; Tokyo; 2011.

[23] Yokozeki T, Kotsuka N, Fujiwara K, Sato T, Yoshimura A, Shoji H. Foreign object impact damage simulation of titanium matrix composites. In: Proceedings of 19th International Conference on Composite Materials, USB; Montreal; 2013.
[24] Ohara Y, Kawashima K. Detection of internal micro defects by nonlinear resonant ultrasonic method using water immersion. Jpn. J. Appl. Phys. 2004;43:3119–3120.

Appendix 1

Plastic constitutive relations used in the numerical simulation are presented herein. Hill and Mises yield functions are used for SiC/Ti and clad layers, respectively. Hill's equivalent stress can be expressed as

$$\bar{\sigma} = \sqrt{F(\sigma_y - \sigma_z)^2 + G(\sigma_z - \sigma_x)^2 + H(\sigma_x - \sigma_y)^2 + 2L\tau_{yz}^2 + 2M\tau_{zx}^2 + 2N\tau_{xy}^2} \quad \text{(A1)}$$

where x, y, and z denote the fiber direction, in-plane transverse direction, and out-of-plane transverse direction, respectively. The following equations are often used to express the anisotropic parameters (e.g. F in Equation (A1)) based on yield stress ratios (e.g. R_{xx}).

$$\begin{gathered} F = \frac{1}{2}\left(\frac{1}{R_{yy}^2} + \frac{1}{R_{zz}^2} - \frac{1}{R_{xx}^2}\right), \quad G = \frac{1}{2}\left(\frac{1}{R_{zz}^2} + \frac{1}{R_{xx}^2} - \frac{1}{R_{yy}^2}\right) \\ H = \frac{1}{2}\left(\frac{1}{R_{xx}^2} + \frac{1}{R_{yy}^2} - \frac{1}{R_{zz}^2}\right), \\ L = \frac{3}{2}\left(\frac{1}{R_{yz}^2}\right), \quad M = \frac{3}{2}\left(\frac{1}{R_{zx}^2}\right), \quad N = \frac{3}{2}\left(\frac{1}{R_{xy}^2}\right) \end{gathered} \quad \text{(A2)}$$

It should be noted that Mises stress corresponds to the case when all the yield stress ratios are 1.

Plastic parameters of SiC/Ti and clad layers were identified based on experimental measurements, although out-of-plane parameters were assumed. The yield stress ratios of SiC/Ti are summarized in Table A1, and these values were input into Marc. The plastic hardening curves (equivalent stress – equivalent plastic strain relations) were input into Marc using the table format which is presented in Table A2 for SiC/Ti and in Table A3 for clad layers.

Table A1. Hill's parameters of SiC/Ti.

R_{xx}	1.0
R_{yy}	0.395
R_{zz}	0.395
R_{yz}	0.395
R_{zx}	0.392
R_{xy}	0.392

Table A2. Hardening curve of SiC/Ti.

Equivalent plastic strain [%]	Equivalent stress [MPa]	Equivalent plastic strain [%]	Equivalent stress [MPa]
0	510	0.09	905
0.01	671	0.1	924
0.02	734	0.2	1089
0.03	780	0.3	1249
0.04	806	0.4	1407
0.05	826	0.45	1466
0.06	848	0.46	1477
0.07	869	0.5	1479
0.08	887	1.0	1481

Table A3. Hardening curve of Ti-6Al-4V clad layers.

Equivalent plastic strain [%]	Equivalent stress [MPa]	Equivalent plastic strain [%]	Equivalent stress [MPa]
0	700	0.35	925
0.025	805	0.4	927
0.05	838	0.5	930
0.1	875	0.815	932
0.15	897	1.14	934
0.2	910	1.51	936
0.25	918	1.70	938
0.3	923	20	940